12

Unsteady Heat Conduction Phenomena in Internal Combustion Engine Chamber and Exhaust Manifold Surfaces

G.C. Mavropoulos
Internal Combustion Engines Laboratory
Thermal Engineering Department, School of Mechanical Engineering
National Technical University of Athens (NTUA)
Greece

1. Introduction

Heat transfer to the combustion chamber walls of internal combustion engines is recognized as one of the most important factors having a great influence both in engine design and operation (Annand, 1963; Assanis & Heywood, 1986; Heywood, 1988; Rakopoulos et al., 2004). Research efforts concerning conduction heat transfer in reciprocating internal combustion engines are aiming, among other, to the investigation of thermal loading at critical combustion chamber components (Keribar & Morel, 1987; Rakopoulos & Mavropoulos, 1996) with the target to improve their structural integrity and increase their factor of safety against fatigue phenomena. The application of ceramic materials in low heat rejection (LHR) engines (Rakopoulos & Mavropoulos, 1999) is also among the large amount of examples where engine conduction heat transfer is a dominant factor. At the same time, special engine cases like the air-cooled (Perez-Blanco, 2004; Wu et al., 2008) or HCCI ones demand a special treatment for a successful description of the heat transfer phenomena involved.

Today, technology changes in the field of the internal combustion engines (mainly the diesel ones) are happening extremely fast. New demands are added towards the areas of controlled ignition of new and alternative fuels (Demuynck et al., 2009), reduction of tailpipe emissions (Rakopoulos & Hountalas, 1998) and improved engine construction that would ensure operation under extreme combustion chamber pressures (well above 200 bar). However, application of these revolutionary technologies creates several functional and construction problems and engine heat transfer is holding a significant share among them. Engine heat transfer phenomena are unsteady (transient), three-dimensional, and subject to rapid swings in cylinder gas pressure and temperatures (Mavropoulos et al., 2008), while the combustion chamber itself with its moving boundaries adds further to this complexity. In modern downsized diesel engines, the extreme combustion pressure and temperature values combined with increased speed values lead to increased amplitude of temperature oscillations and thus to enormous thermal loading of chamber surfaces (Rakopoulos et al., 1998). At the same time, transient engine operation (changes of speed and/or load) imposes a significant additional influence to the system heat transfer, which cannot (and should not)

be neglected during the engine design stage (Mavropoulos, 2011). It is obvious that there is an urgent demand for simple and effective solutions that would allow the new technologies to enter marketplace as quick as possible. Likely, there are also available today several important tools (both theoretical and experimental) that help a lot the researchers towards solution of the above described problems.

Phenomena related to unsteady internal combustion engine heat transfer belong in two main categories:

- Short-term response ones, which are caused by the fluctuations of gas pressure and temperature during an engine cycle. As a result, temperature and heat flux oscillations are caused in the surface layers of combustion chamber in the frequency of the engine operating cycle (thus having a time period in the order of milliseconds). These are otherwise called cyclic engine heat transfer phenomena.
- Long-term response ones, resulting from the large time scale (in the order of seconds), non-periodic variations of engine speed and/or load. As a result, thermal phenomena of this category occur only during the transient engine operation. On the other hand, the short-term response phenomena are present under both engine operating modes.

Both the above categories of engine transient heat transfer phenomena have been investigated by the present author (Mavropoulos et al., 2009; Mavropoulos, 2011) and also other research groups. In (Keribar & Morel, 1987) the authors have studied the development of long-term temperature variations after a load or speed change. They used a convective heat transfer submodel based on in-cylinder flow accounting for swirl, squish, and turbulence, and a radiation heat transfer submodel based on soot formation.

Despite the large amount of existing studies with reference to the two categories of engine heat transfer phenomena, there is limited information (a few papers only) which examine both long- and short-term response categories together at the same time. In (Lin & Foster, 1989) the authors have reported experimental results concerning cycle resolved cylinder pressure, surface temperature and heat flux for a diesel engine during a step load change. They have also developed an analysis model to calculate heat flux during transient. In (Wang & Stone, 2008) the authors have studied the engine combustion, instantaneous heat transfer and exhaust emissions during the warm-up stage of a spark ignition engine. An one-dimensional model has been used to simulate the engine heat transfer during the warm-up stage. They have reported an increase in the measured peak heat flux as the combustion chamber wall temperature rises during warm-up.

However, several important issues still today remain under investigation. For example, and despite the significant progress made in this area during the last years (Mavropoulos et al., 2008, 2009; Mavropoulos, 2011) the interaction between long-term non-periodic variation of combustion chamber temperature caused during the transient engine operation and the short-term cyclic fluctuations of surface temperatures and heat fluxes needs to be further elucidated. It is of utmost importance to describe in detail, among other issues, the effect of this interaction on peak pressure, on the amplitude and phase change of temperature and heat flux oscillations etc. The answers to these questions would also reveal in what extend the transient heat transfer phenomena should be accounted for during the early design stage of an engine. In addition it needs to be clarified if the specific characteristics (time period, percentage of load and speed change) of any engine transient event influence the mechanism and characteristics of unsteady heat conduction in combustion chamber walls. An attempt to provide some insight to the above important phenomena would be performed by the author among other issues, in the present paper.

A special part of engine heat transfer studies concerns the gas exchange system. The phenomena of transient heat transfer in the intake and exhaust engine manifolds are of special difficulty due to the complex dynamic nature of gas flow inside both of them. Many interesting developments have been recently reported in (Sammut & Alkidas, 2007). An attempt to explore the combination of both short- and long-term unsteady conduction heat transfer effects in the exhaust manifold would also be among the subjects of the present paper.

The present author is participating as the main researcher in a general research program aiming to the investigation of heat transfer phenomena as they are developed in the Internal Combustion Engine chamber and exhaust manifold surfaces. This program was initiated more than fifteen years ago in the Internal Combustion Engine Laboratory (ICEL) of NTUA and is still today under progress. Within this framework, he has already reported detailed structural and thermodynamic analysis models (Rakopoulos & Mavropoulos, 1996), which are also capable to take into account the heat transfer behaviour of the insulated engine (Rakopoulos & Mavropoulos, 1998). He has also reported in detail the short-term variation of instantaneous diesel engine heat flux and temperature during an engine cycle (Rakopoulos & Mavropoulos, 2000, 2008, 2009). Among the most significant accomplishments of this investigation is the detailed description of the different phases of unsteady heat transfer and their accompanied phenomena as they are developed in the combustion chamber and exhaust manifold surfaces during an engine transient event. In addition, a prototype experimental measuring installation has been developed, specially configured for the investigation of the complex engine heat transfer phenomena. Using this installation they have been obtained experimental data during transient engine operation simultaneously for long- and short-term heat transfer variables' responses as they are developed in the internal surfaces of the combustion chamber. Similar experimental data have been obtained by the author and were presented for the first time in the relevant literature also from the exhaust manifold surfaces during transient engine operation (Mavropoulos et al., 2009; Mavropoulos, 2011).

In the present book chapter an overview is provided concerning several of the most important findings of engine heat transfer research as it was realized during a series of years in ICEL Laboratory of NTUA. It is especially examined the influence of transient engine operation (change of speed and/or load) on the short-term response cyclic oscillations as they are developed in the surface layers of combustion chamber and exhaust manifold. Among the factors influencing heat transfer, in the present investigation the effect of severity of the transient event as well as issues related with local heat transfer distribution would be considered. It is clearly displayed and quantified the significant influence of a transient event of speed and load change on engine cyclic temperatures and heat fluxes both for engine cylinder and exhaust manifold. Two phases (a thermodynamic and a structural one) are clearly distinguished in a thermal transient and the cases where such an event could endanger the engine structural integrity are emphasized.

2. Simulation model for unsteady wall heat conduction

2.1 Modelling cases

It should be emphasized that in the present work they are concerned only the phenomena related to unsteady engine heat transfer which present the highest degree of interest. Thus

several heat transfer phenomena and corresponding modelling cases applicable to steady-state engine operation would not be mentioned in the following.
Under the above framework, the prediction of the temperature distribution in the metallic parts of combustion chamber involves the solution of the unsteady heat conduction equation with the appropriate boundary conditions. The following two different simulation cases were considered leading to the development of respective models:

a. Three-dimensional Finite Element (FEM) model developed and used for the overall description of thermal field as it is developed during a transient event in combustion chamber components. This is mainly applicable for the investigation of the long-term heat transfer phenomena which are extended throughout the whole volume of each component. However it can be as equally used for the investigation of the heat transfer phenomena developed in the short-term scale.
b. One-dimensional heat conduction model developed and used for the calculation of instantaneous heat flux through a certain location of the combustion chamber wall. This is only applicable for the investigation of heat transfer phenomena developed in the short-term scale which influence exclusively the surface layers of each component (the ones in contact with combustion gases) up to a distance of a few mm inside its metal volume.

Both previous models give satisfactory results with significant computer time economy. Boundary conditions are assumed to be of all three kinds, i.e. constant surface temperature, constant heat flux or constant heat-transfer coefficient and surrounding fluid temperature (convective conditions). Their successful application depends on the correct knowledge of the physical mechanisms that take place on the gas and cooling sides of the various combustion chamber parts. Details on all previous topics can be found in (Rakopoulos & Mavropoulos, 1996, 1998).

2.2 Three-dimensional FEM analysis of transient temperature fields

The heat conduction equation for a three-dimensional axisymmetric, time-dependent, problem takes the form (in the absence of heat sources and for constant thermal conductivity):

$$\frac{\partial T}{\partial t} = \frac{k}{\rho \cdot c}\left(\frac{\partial^2 T}{\partial r^2} + \frac{1}{r}\frac{\partial T}{\partial r} + \frac{\partial^2 T}{\partial z^2} \right) \tag{1}$$

The development of a Finite-Element formulation for the unsteady heat conduction equation with all three kinds of boundary conditions, was based on a "variational" approach i.e. minimization of an appropriate variational statement. This is a standard and well known procedure (Rakopoulos & Mavropoulos, 1996) leading for the unsteady heat conduction case to the following system of differential equations:

$$[C][\dot{T}] = -\left[[K] + [H_s]\right][T] + [h_s] + [q_s] \tag{2}$$

with the additional assumption of linear temperature variation inside every finite element.
Following an "element by element" analysis and summing up over the whole region of interest, we obtain the final expression of the characteristic matrices (conduction, convection, heat flux etc.) as they are used in eq. (2). The procedure has been presented in detail in (Rakopoulos & Mavropoulos, 1996).

2.3 Boundary conditions at the combustion chamber components

A variety of thermal boundary conditions is necessary to complete the application of FEM models for the prediction of temperature and heat flux distributions on engine structure. Since the application of these conditions introduces a factor of uncertainty onto the final results, a detailed knowledge of the physical mechanisms becomes essential. To overcome these difficulties the author have tested with success and presented in the past (Rakopoulos & Mavropoulos, 1996) a detailed set of boundary conditions for all combustion chamber surfaces. For the gas-side of combustion chamber components, the analysis of experimental pressure measurements results to the calculation of the instantaneous values for heat transfer coefficient h_g and temperature T_g as a function of crank angle. From these, the time averaged equivalent values can be calculated for a four-stroke engine:

$$\bar{h}_g = \frac{1}{4\pi}\int_0^{4\pi} h_g d\phi \quad , \quad \bar{T}_g = \frac{1}{4\pi \bar{h}_g}\int_0^{4\pi} T_g h_g d\varphi \tag{3}$$

Special attention is needed when modelling the boundary conditions at the piston-ring-liner interfaces through which a large quantity of heat passes, under low thermal resistance conditions. Any attempt to evaluate a heat transfer coefficient between skirt and liner and especially between rings and ring-grooves requires a complete knowledge of dimensions and clearances among them. Following this information, two basic assumptions were made: (a) Flow through crevices is a fully developed laminar one (Couette), and (b) Clearances in the above areas are very small and as a result convection mechanisms can be neglected.

At the piston top land part and the lower part of skirt the heat transfer coefficient is mainly determined by the magnitude of the radial clearance (Δx) of the gas or oil film between piston and liner. For the various surfaces of the ring belt, however, a thermal network model was adopted and the corresponding thermal circuits were created for the upper, lower and side surface of each ring-groove, respectively.

For the piston undercrown surface, the heat transfer coefficient depends strongly on the piston design and cooling system used. For the majority of calculation cases a jet piston cooling is adopted, so that the heat transfer coefficient is calculated by the expression:

$$h_{oil} = 68.17\left[(r\omega)\frac{D_n}{\nu_b}\right]^{1/2} \quad (W/m^2K) \tag{4}$$

where h_{oil} is the heat transfer coefficient between oil and undercrown surface, r is the crank radius, D_n is the nozzle diameter of oil sprayer in m, ν_b is the oil kinematic viscosity at bulk oil temperature in m^2/sec and ω the engine angular speed.

In the case of air cooled engines the fins at the outside surface of cylinder head and liner form a number of parallel closed cooling passages via the cowling; here for the estimation of heat transfer coefficient Nusselt-type equations are considered, depending on the state of flow as follows:

a. For laminar flow with Reynolds numbers less than 2100 the Nusselt-type relation, based on the work by Sieder and Tate is (Annand, 1963)

$$Nu = 1.86\left[Re\,Pr\frac{D_1}{L}\right]^{1/3}\left(\frac{\mu_b}{\mu_s}\right)^{0.14} \tag{5}$$

where the air properties are evaluated at the bulk 'b' temperature which is the arithmetic mean of the inlet and outlet temperatures, whereas subscript 's' refers to the surface temperature. In addition, L is the length of the flow path and D_1 is the equivalent hydraulic diameter, $D_1 = 4A/f$, where A is the flow surface area in each cooling passage and f its internal (cooling) perimeter.

b. For the transition region with Reynolds numbers ranging from 2100 to 10000 the Nusselt-type relation, based on the work by Hausen is

$$Nu=0.116\left[Re^{2/3}-125\right]Pr^{1/3}\left(\frac{\mu_b}{\mu_s}\right)^{0.14}\left[1+\left(\frac{D_1}{L}\right)^{2/3}\right] \quad (6)$$

with the same symbol meanings as for the previous case, and

c. For turbulent flow with Reynolds numbers greater than 10000 the Nusselt-type relation, based on the work by Sieder and Tate is

$$Nu = 0.023\left(Re\right)^{0.8}Pr^{1/3}\left(\frac{\mu_b}{\mu_s}\right)^{0.14} \quad (7)$$

It is obvious from equations (5) to (7) that the air velocity through the engine fins is the most important factor in the engine cooling process. A detailed theoretical study in correlation with experimental results is necessary in order to determine the most accurate values of heat transfer coefficient for the particular engine type and operating conditions in hand.

2.4 One-dimensional unsteady wall heat conduction at surface layers

For the calculation of instantaneous heat flux through a certain location of the combustion chamber wall for a complete engine cycle during steady state operation, the time periodic (unsteady) heat conduction model is used. In this case, Fourier analysis is the standard calculation procedure as it is well-established by the present author (Mavropoulos et al., 2008, 2009; Mavropoulos, 2011) and other research groups (Demuynck et al., 2009). However, for the case of the transient engine operation the heat transfer phenomena that occur in combustion chamber (and also in exhaust manifold) surfaces are dynamic (that is time dependent) but non-periodic. So in that case, the basic assumption for the application of Fourier method, that is a time periodic problem, is not valid anymore.

To overcome this difficulty, the author has developed a modified version of Fourier analysis. Its basic principles have been described in detail in (Mavropoulos et al., 2009). It is based on the idea of separation of the continuous transient variation from its initial until its final steady state to a number of discrete steps N_c, each of them having the duration of the corresponding engine cycle. In other words, each engine cycle is decoupled from the rest of the transient event. Having adopted this approximation, each individual engine cycle is considered to be repeated for an infinite number of times, so that heat flow through the corresponding component becomes time periodic and thus Fourier analysis can be finally applied. It has been already validated from the results presented in (Mavropoulos et al., 2009) that such an approximation does not impose any significant errors.

Assuming that heat flow through the component is one-dimensional and that material properties remain constant, the corresponding expression of the unsteady heat conduction equation for the i-th cycle of the transient event is given by

$$\left(\frac{\partial T}{\partial t}=\alpha\frac{\partial^2 T}{\partial x^2}\right)_i \tag{8}$$

where i=1,…,Nc with Nc the total number of engine cycles during a transient event of engine speed and/or load change. Additionally, x is in this case the distance from the wall surface, $\alpha=k_w/\rho_w c_w$ is the wall thermal diffusivity, with ρ_w the density and c_w the specific heat capacity.

Following the steps used in the classic heat conduction Fourier analysis as presented in (Mavropoulos et al., 2008, 2009), the following expression is reached for the calculation of instantaneous heat flux on the combustion chamber surfaces during the transient engine operation

$$\begin{aligned} q_{w,i}(t)&=\left(-k_w\left.\frac{\partial T}{\partial x}\right|_{x=0}\right)_i=\frac{k_w}{\delta}\left(T_{m,i}-\overline{T}_{\delta,i}\right)+\\ &k_w\sum_{n=1}^{N}\phi_{n,i}\left[\left(A_{n,i}+B_{n,i}\right)\cos(n\omega_i t)+\left(B_{n,i}-A_{n,i}\right)\sin(n\omega_i t)\right]\end{aligned} \tag{9}$$

where δ is the distance from the wall surface of the in-depth thermocouple. Additionally, $T_{m,i}$ is the time averaged value of wall surface temperature $T_{w,i}$, $A_{n,i}$ and $B_{n,i}$ are the Fourier coefficients all of them for the i-th cycle, n is the harmonic number, N is the total number of harmonics, and ω_i (in rad/s) is the angular frequency of temperature variation in the i-th cycle, which for a four-stroke engine is half the engine angular speed. In the developed model, there is the possibility for the total number of harmonics N to be changed from cycle to cycle in case such a demand is raised by the form of temperature variation in any particular cycle.

3. Categories of unsteady heat conduction phenomena

Phenomena related to unsteady heat conduction in Internal Combustion Engines are often characterized in literature with the general term "thermal transients". In reality these phenomena belong to different categories considering their development in time. As a result and for systematic reasons a basic distribution is proposed for them as it appears in Fig. 1.

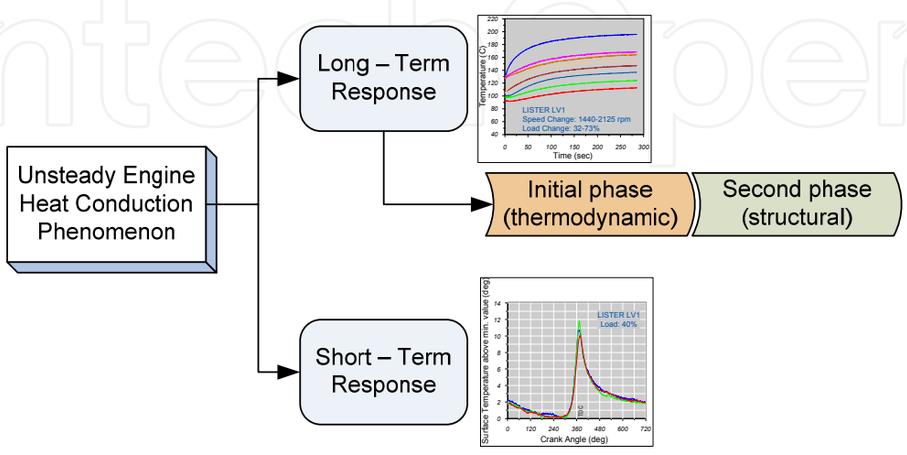

Fig. 1. Categories of engine unsteady heat conduction phenomena.

As observed any unsteady engine heat transfer phenomenon belongs in either of the following two basic categories:

- Short-term response ones, which are caused by the fluctuations of gas pressure and temperature during an engine cycle. These are otherwise called cyclic engine heat transfer phenomena and are developing during a time period in the order of milliseconds. Phenomena in this category are the result of the physical and chemical processes developing during the period of an engine cycle. They are finally leading to the development of temperature and heat flux oscillations in the surface layers of combustion chamber components. It is noted here that phenomena in this category should not normally mentioned as "transient" since they are mainly related with "steady state" engine operation. However their presence during transient engine operation is as equally important and this is considered in the present work. In addition the oscillating values of heat conduction variables around the surfaces of combustion chamber present a "transient" distribution in space since they are gradually faded out until a distance of a few mm below the surface of each component.
- Long-term response ones, resulting from the large time scale non-periodic variations of engine speed and/or load. As a result, thermal phenomena of this category have a time "period" in the order of several hundreds of seconds and are presented only during the transient engine operation.

Each case of long-term response thermal transient can be further separated in two different phases (Figs 1 and 2). The first of them involves the period from the start of variation until the instant in which all thermodynamic (combustion gas pressure and temperature, gas mixture composition etc.) and functional variables (engine torque, speed) reach their final state of equilibrium. This period lasts a few seconds (usually 3-20) depending on the type of engine and also on the kind of transient variation under consideration. This first phase of thermal transient is named as "thermodynamic".

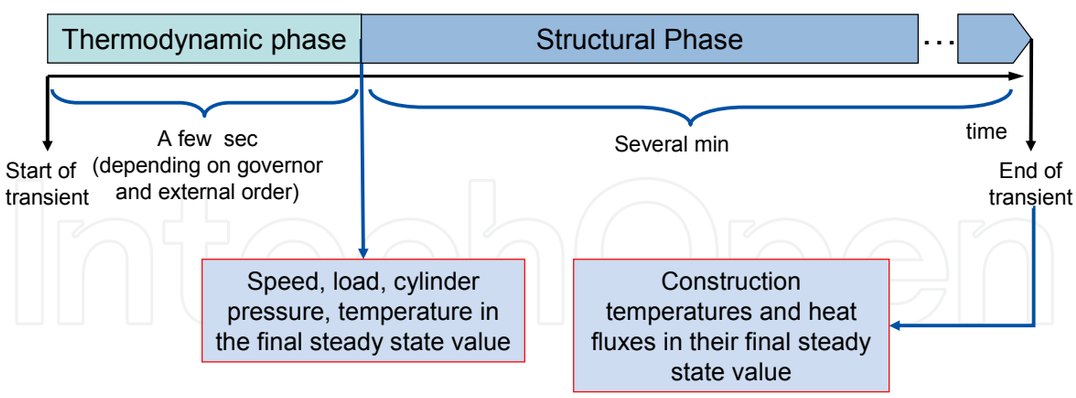

Fig. 2. Phases of long term response thermal transient event.

The upcoming second phase of the transient thermal variation is named as "structural" and its duration could in some cases overcome the 300 sec until all combustion chamber components have reached their temperatures corresponding to the final steady state. In the end of this second phase all variables related with heat conduction in the combustion chamber (temperatures, heat fluxes) and all heat transfer parameters of the fluids surrounding the combustion chamber (water, oil etc.) have reached their values corresponding to the final state of engine transient variation.

Specific examples from the above thermal transient variations are provided in the upcoming sections.

4. Test engine and experimental measuring installation

4.1 Description of the test engine

A series of experiments concerning unsteady engine heat transfer was conducted by the author on a single cylinder, Lister LV1, direct injection, diesel engine. The technical data of the engine are given in Table 1. This is a naturally aspirated, air-cooled, four-stroke engine, with a bowl-in-piston combustion chamber. All the combustion chamber components (head, piston, liner etc.) are made from aluminum. The normal speed range is 1000-3000 rpm. The engine is equipped with a PLN fuel injection system. A three-hole injector nozzle (each hole having a diameter of 0.25 mm) is located in the middle of the combustion chamber head. The engine is permanently coupled to a Heenan & Froude hydraulic dynamometer.

Engine type	Single cylinder, 4-stroke, air-cooled, DI
Bore/Stroke	85.73 mm/82.55 mm
Connecting rod length	148.59 mm
Compression ratio	18:1
Speed range	1000-3000 rpm
Cylinder dead volume	28.03 cm^3
Maximum power	6.7kW @ 3000 rpm
Maximum torque	25.0 Nm @ 2000 rpm
Inlet valve opening/ closing	15^{o}CA before TDC /41^{o}CA after BDC
Exhaust valve opening /closing	41^{o}CA before BDC /15^{o}CA after TDC
Inlet / Exhaust valve diameter	34.5mm / 31.5mm
Fuel pump	Bryce-Berger with variable-speed mechanical governor
Injector	Bryce- Berger
Injector nozzle opening pressure	190 bar
Static injection timing	28^{o}CA before TDC
Specific fuel consumption	259 g/kWh (full load @ 2000 rpm)

Table 1. Engine basic design data of Lister LV1 diesel engine.

The engine experimental test bed was accompanied with the following general purpose equipment:

- Rotary displacement air-flow meter for engine air flow rate measurement
- Tank and flow-meter for diesel fuel consumption rate measurement
- Mechanical rpm indicator for approximate engine speed readings
- Hydraulic brake water pressure manometer, and
- Hydraulic brake water temperature thermometer.

4.2 Experimental measuring installation

4.2.1 General

A detailed description of the experimental installation that was used in the present investigation can be found in previous publications of the author (Mavropoulos et al., 2008,

2009; Mavropoulos, 2011). For that reason, only a brief description will be provided in the following.

The whole measuring installation was developed by the author in the ICEL Laboratory of NTUA and was specially designed for addressing internal combustion engine thermal transient variations (both short- and long-term ones). As a result, its configuration is based on the separation of the acquired engine signals into two main categories:

- Long-term response ones, where the signal presents a non-periodic variation (or remains essentially steady) over a large number of engine cycles, and
- Short-term response ones, where the corresponding signal period is one engine cycle.

To increase the accuracy of measurements, the two signal categories are recorded separately via two independent data acquisition systems, appropriately configured for each one of them. For the application in transient engine heat transfer measurements, the two systems are appropriately synchronized on a common time reference.

4.2.2 Long-term response installation

The long term response set-up comprises 'OMEGA' J- and K-type fine thermocouples (14 in total), installed at various positions in the cylinder head and liner in order to record the corresponding metal temperatures. Nine of those were installed on various positions and in different depths inside the metal volume on the cylinder head and they are denoted as "TH#j" (j=1,…9) in Fig. 3 (a and b). Thermocouples of the same type were also used for measuring the mean temperatures of the exhaust gas, cooling air inlet, and engine lubricating oil.

The extensions of all thermocouple wires were connected to an appropriate data acquisition system for recording. A software code was written in order to accomplish this task.

4.2.3 Short-term response installation

The short-term response installation is in general the most important as far as the periodic thermal phenomena inside the engine operating cycle are concerned. In general, it presents the greater difficulty during the set-up and also during the running stage of the experiments. It comprises the following components:

4.2.3.1 Transducers and heat flux probes

The following transducers were used to record the high-frequency signals during the engine cycle:

- "Tektronix" TDC marker (magnetic pick-up) and electronic 'rpm' counter and indicator.
- "Kistler" 6001 miniature piezoelectric transducer for measuring the cylinder pressure, flush mounted to the cylinder head. Its output signal is connected to a "Kistler" 5007 charge amplifier.
- Four heat flux probes installed in the engine cylinder head and the exhaust manifold, for measuring the heat flux losses at the respective positions. The exact locations of these probes (HT#1 to 4) and of the piezoelectric transducer (PR#1), are shown in the layout graph of Fig. 3a and also in the image of Fig. 3b.

The prototype heat flux sensors were designed and manufactured by the author at the Internal Combustion Engine Laboratory (ICEL) of (NTUA). Additional details and technical data about them can be found in (Mavropoulos et al., 2008, 2009). They are customized

especially for this application as shown in the images of Fig. 4 where it is presented the whole instantaneous heat flux measurement system module created and used for the present investigation. They belong in two different types as described below:

- Heat flux sensors (HT#1-3 in Fig. 3a and 3b) installed on the cylinder head, consisting of a fast response, K-type, flat ribbon, "eroding" thermocouple, which was custom designed and manufactured for the needs of the present experimental installation, in combination with a common K-type, in-depth thermocouple. Each of the fast response thermocouples was afterwards fixed inside a corresponding compression fitting, together with the in-depth one that is placed at a distance of 6 mm apart, inside the metal volume. The final result is shown in Fig. 4.

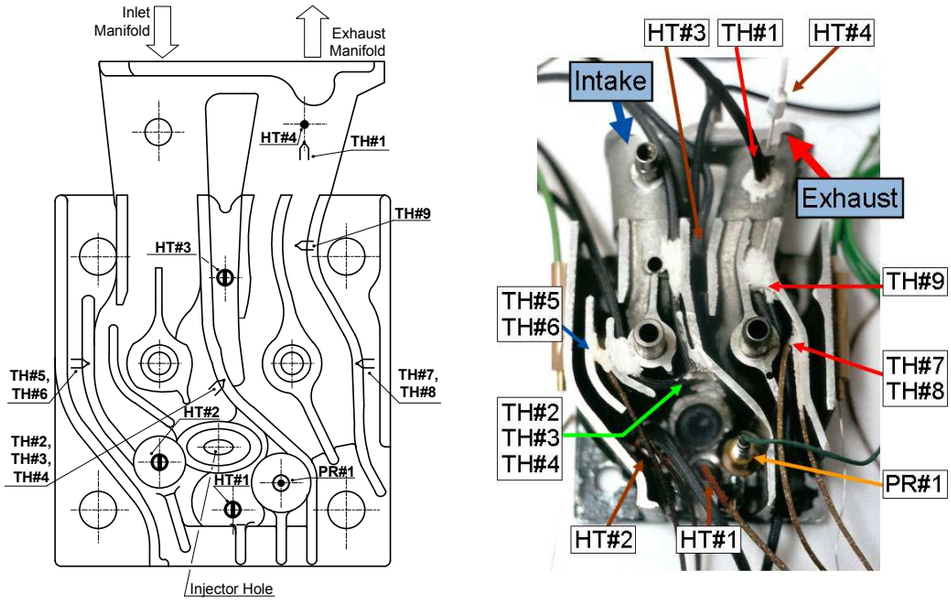

Thermoc. #	Distance from top head surface (mm)
TH#1	0.0
TH#2	53.4
TH#3	18.0
TH#4	4.0
TH#5	21.0
TH#6	4.0
TH#7	21.0
TH#8	5.0
TH#9	0.0

(a)

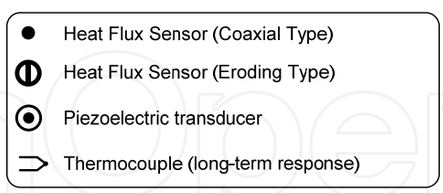

(b)

Fig. 3. Graphical layout (a), and image (b), of the engine cylinder head instrumented with the surface heat flux sensors, the piezoelectric pressure transducer and the "long-term" response thermocouples at selected locations.

- The heat flux sensor installed in the exhaust manifold (HT#4 in Fig. 3a and 3b) has the same configuration, except that the fast response thermocouple used is a J-type, "coaxial" one. It is accompanied with a common J-type, in-depth thermocouple, located inside the compression fitting at a distance of 6 mm behind it. The sensor was flush-mounted on the exhaust manifold at a distance of 100 mm (when considered in a straight line) from the exhaust valve.

The heat flux sensors developed in this way displayed a satisfactory level of reliability and durability, necessary for this application. Also, special care was given to minimize distortion of thermal field in each position caused by the presence of the sensor. Before being placed to their final position in the cylinder head and exhaust manifold, all heat flux sensors were extensively tested and calibrated through a long series of experiments conducted in different engines, under motoring and firing operating conditions.

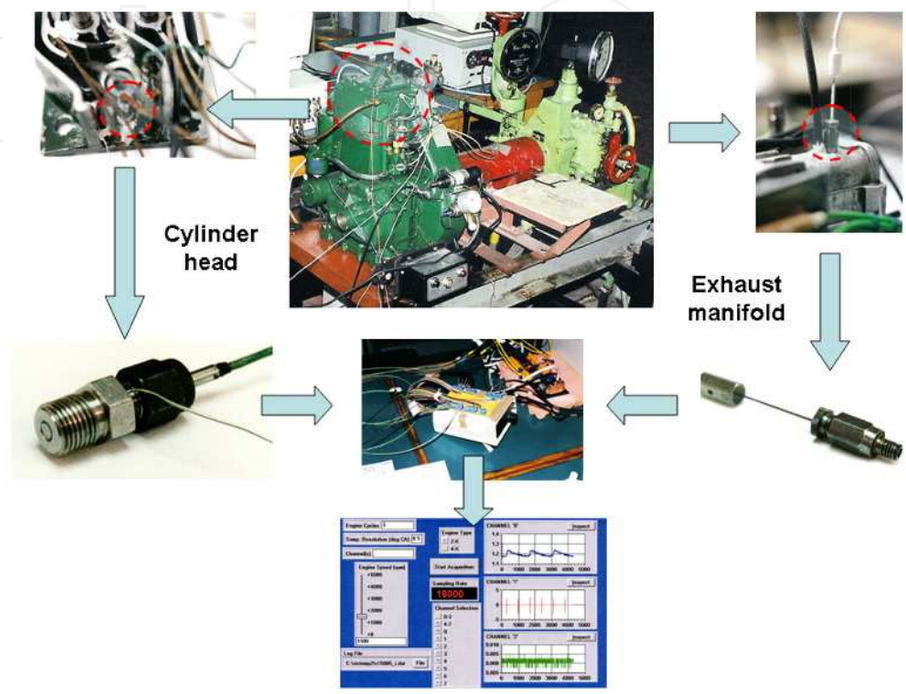

Fig. 4. Instantaneous heat flux measurement system module used in the cylinder head and exhaust manifold wall.

4.2.3.2 Signal pre-amplification and data acquisition system

In order to obtain a clear thermocouple signal when acquiring fast response temperature and heat flux data, the author had introduced the technique of an initial pre-amplification stage. This independent pre-amplification stage is applied on the sensor signal before the latter enters the data acquisition system. The need for such an operation emanates from the fact that this kind of measurements combines the low voltage level of a thermocouple signal output with an unusual high frequency. As a result, its direct acquisition using a common multi-channel data acquisition system creates a great percentage of uncertainty and in some cases it becomes even impossible. The introduction of pre-amplification stage solves the previous problems with only a small contribution to signal noise. For recording the fast response signals during the transient engine operation, the frequency used was in the range of 4500-6000 ksamples/sec/channel, which resulted in a corresponding signal resolution in the range of 1-2 deg CA dependent on the instantaneous engine speed.
The prototype preamplifier and signal display device (Fig. 4) was designed and constructed in the NTUA-ICEL laboratory, using commercially available independent thermocouple amplifier modules for the J- and K-type thermocouples, respectively. Ten of the above amplifiers were installed on a common chassis together with necessary selectors and

displays, forming a flexible device that can route the independent heat flux sensor signals either in the input of an oscilloscope for display and observation, or in the data acquisition system for recording and storage as it is displayed in Fig. 4. Additional details for the pre-amplifier can be found in (Mavropoulos et al., 2008, 2009, Mavropoulos, 2011). After the development of this device by the author, similar devices specialized in fast response heat flux signal amplification have also become commercially available.
The output signals from the thermocouple pre-amplifier unit, together with the magnetic TDC pick-up and piezoelectric transducer signals are connected to the input of a high-speed data acquisition system for recording. Additional details concerning the data acquisition system are provided in (Mavropoulos, 2011).

5. Presentation and discussion of the simulated and experimental results

5.1 Simulation process and experimental test cases considered

The theoretical investigation of phenomena related to the unsteady heat conduction in combustion chamber components was based on the application of the simulation model for engine performance and structural analysis developed by the author. The structural representation of each component is based on the 3-dimensional FEM analysis code developed especially for the simulation of thermal phenomena in engine combustion chamber. For the application of boundary conditions in the various surfaces of each component, a series of detailed physical models is used. As an example, for the boundary conditions in the gas side of combustion chamber a thermodynamic simulation model of engine cycle operation is used in the degree crank angle basis. A brief reference of the previous models was provided in subsections 2.2 and 2.3. Additional details are available in previous publications (Rakopoulos & Mavropoulos, 1996, 1999).
Like any other classic FEM code, the thermal analysis program developed consists of the following three main stages: (a) preprocessing calculations; (b) main thermal analysis; and (c) postprocessing of the results. An example of these phases of solution is provided in Fig. 5 (a-e) applied in an actual piston and liner geometry of a four stroke diesel engine. For each of the components a 3-dimensional representation (Fig. 5a) is first created in a relevant CAD system. In the next step the component is analysed in a series of appropriate 3d finite elements (Fig. 5b) and the necessary boundary conditions are applied in all surfaces. Then, during the main analysis the thermal field in each component is solved and this process could follow several solution cycles until an acceptable convergence in boundary conditions is achieved. It should be mentioned in this point that due to the complex nature of this application each combustion chamber component is not independent but it is in contact with others (for example the piston with its rings and liner etc.). This way the final solution is achieved when the heat balance equation between all components involved is satisfied. More details are provided in (Rakopoulos & Mavropoulos, 1998, 1999).
For the postprocessing step one option is a 3d representation of the thermal field variables (Fig. 5c and 5d). In alternative, a section view (Fig. 5e) is used to describe the thermal field in the internal areas of the structure in detail. This way the comparison with measured temperatures in specific points of the component (numbers in parentheses in Fig. 5e) is also available which is used for the validation of the simulated results.
For the needs of the present investigation several characteristic actual engine transient events were selected to demonstrate the results of the unsteady heat conduction simulation model both in the long-term and in the short-term time scale. All of them are performed in

the test engine and the experimental installation described in section 4. For the long-term scale the following two variations are examined:

- A load increment (*"variation 1"*) from an initial steady state of 2130 rpm engine speed and 40% of full load to a final one of 2020 rpm speed and 65% of full load.

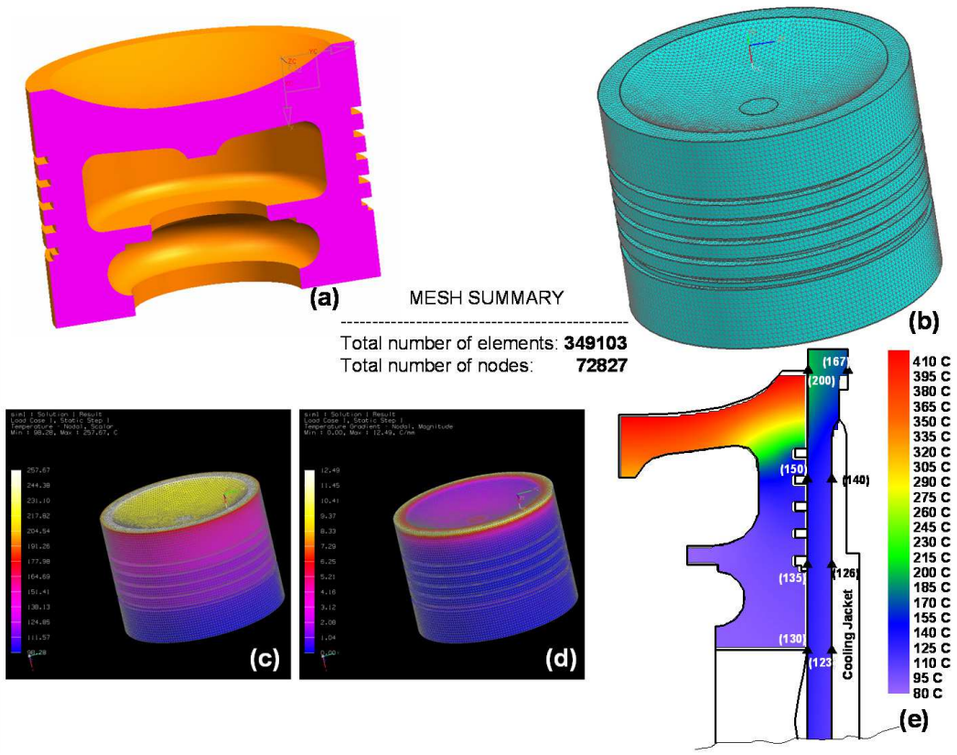

Fig. 5. Application of the simulation model for engine performance and structural analysis. A 3d engine piston geometry representation (a), its element mesh (b) and results of thermal field variables in three (c and d) and two dimensional representations (e).

- A speed increment (*"variation 2"*) from an initial steady state of 1080 rpm engine speed and 10% of full load to a final one of 2125 rpm speed and 40% of full load.

For the short-term scale the next two transient events are respectively considered:

- A change from 20-32% of full load *("variation 3")*. During this change, engine speed remained essentially constant at 1440 rpm. Characteristic feature in this variation was the slow pace by which the load was imposed (in 10 sec, approximately). For this transient variation, a total of 357 consecutive engine cycles were acquired in a 30 sec period via the "short-term response" system signals. For the "long-term response" data acquisition system, the corresponding figures for this transient variation raised in 3417 consecutive engine cycles during a time period of 285 sec.
- Following the previous one, a change from 32-73% of full engine load *("variation 4")* with a simultaneous increase in engine speed from 1440 to 2125 rpm. In this variation, the load change was imposed rapidly in an approximate period of 2 sec. This was accomplished on purpose trying to imitate in the "real engine" the theoretical *ramp* variation of engine speed and load. For this transient variation and the "short-term response" system, 695 engine cycles were acquired in a period of 40 sec. The

corresponding figures for the "long-term response" signals raised in 5035 engine cycles in a time period of 285 sec.

For all the above transient variations, the initial and final steady state signals were additionally recorded from both the short- and long-term response installations. Selective results from the simulation performed and the experiments conducted concerning the previous four variation cases are presented in the upcoming sections.

5.2 Results concerning long-term heat transfer phenomena in combustion chamber

Before proceeding with the application of the model to transient engine operation cases, it was first necessary to calibrate the thermostructural submodel under steady state conditions, especially for the verification of the application of boundary conditions as described in 2.3. Several typical transient variations (events) of the engine in hand were then examined which involve increment or reduction of load and/or speed. Results concerning variation of engine performance variables under each transient event are not presented at the present work due to space limitations. They are available in existing publications of the author (Mavropoulos et al., 2009; Rakopoulos et al., 1998; Rakopoulos & Mavropoulos, 2009).

The Finite Element thermostructural model was then applied for the cylinder head of the Lister-LV1, air-cooled DI diesel engine for which relevant experimental data are available. For the needs of the present application a mesh of about 50000 tetrahedral elements was developed, allowing a satisfactory degree of resolution for the most sensitive points of the construction like the valve bridge area. For the early calculation stages it was found convenient to utilize a coarser mesh, which helps on the initial application of boundary conditions furnishing significant computer time economy. The final finer mesh can then be applied giving the maximum possible accuracy on the final result.

In Fig. 6a the experimental temperature values taken from three of the cylinder head thermocouples (TH#2-TH#4) during the load increment variation "1", are compared with the corresponding calculated ones at the same positions. The calculated curves follow satisfactorily the experimental ones throughout the progress of the transient event. The steepest slope between the different curves included in Fig. 6a is observed on the corresponding ones of thermocouple TH#2 (Fig. 3) placed at the valve bridge area, while the most moderate one is observed for thermocouple TH#4 placed at the outer surface of the cylinder head. As expected, the valve bridge is one of the most sensitive areas of the cylinder head suffering from thermal distortion caused by these sharp temperature gradients during a transient event (thermal shock). Many cases of damages in the above area have been reported in the literature, a fact which also confirms the results of the present calculations.

Similar observations can be made for the cylinder head temperatures in the case of the speed increment variation "2" presented in Fig. 6b. Again the coincidence between calculated and experimental temperature profiles is very good. Temperature levels for all positions present now smaller differences between the initial and final steady state; the steepest temperature gradient is again observed in the valve bridge area. The initial drop in the temperature value of thermocouple TH#4 is due to the increase in engine speed for the first few seconds of the variation which causes a corresponding increase in the air velocity through the fins and so in the heat transfer coefficient given by eqs (5) to (7) with a simultaneous decrease in air temperature. From the results presented in Fig. 6 it is concluded that the developed model

manages to simulate satisfactorily the long-term response unsteady heat transfer phenomena as they are developed in the engine under consideration.

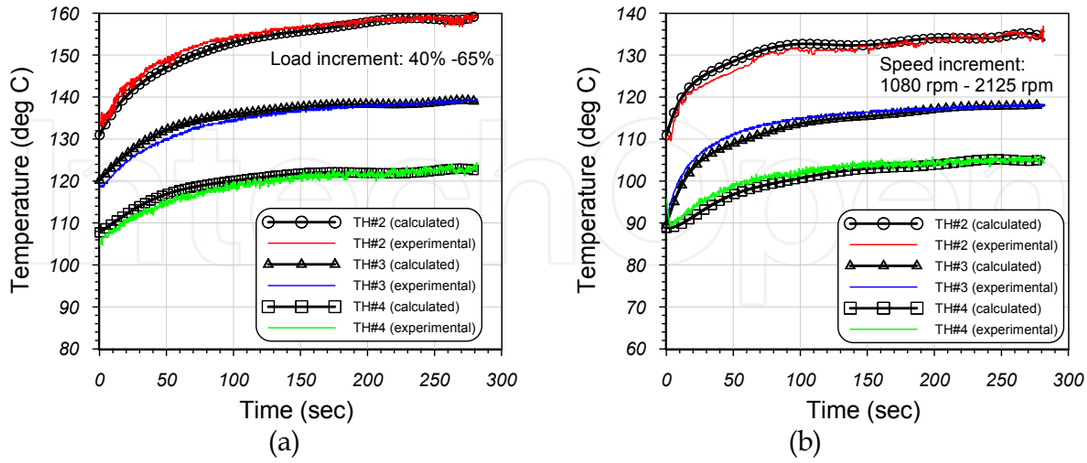

Fig. 6. Comparison between calculated and experimental temperature profiles vs. time for three of the cylinder head thermocouples, during the load increment variation "1" (a) and the speed increment variation "2" (b).

Figs 7 (a and b) present the results of temperature distributions at the whole cylinder head area in the form of isothermal charts, as they were calculated for the initial and final steady state of transient variation "1". Numbers inside squares denote experimental temperature values recorded from thermocouples. A significant degree of agreement is observed between the simulated temperature results and the corresponding measured values which confirms for the validity of the developed model. Similar charts could be drawn for any of the variations examined and at any specific moment of time during a transient event. They are presenting in a clear way the local temperature distinctions in the various parts of the construction, thus they are revealing the mechanism of heat dissipation through the structure. The observed temperature differences between the inlet and the exhaust valve side of the cylinder head (exceeding 150 ^{o}C for the full load case) are characteristic for air-cooled diesel engines, where construction leaves only small metallic common areas between the inlet and the exhaust side of head. Corresponding results reported in the literature confirm the above observation (Perez-Blanco, 2004; Wu et al., 2008).

5.3 Results concerning short-term heat transfer phenomena in combustion chamber

During the experiments conducted, the heat flux sensors HT#2 and HT#3 (installed on the cylinder head) were not able to operate adequately over most of the full spectrum of measurements taken. The reasons for this failure are described in detail in (Mavropoulos et al., 2008). Therefore, in this work the short-term results for the cylinder head will be presented only from sensor HT#1 together with the ones for the exhaust manifold from sensor HT#4.

In Figs 8 and 9 are presented the time histories for several of the most important engine performance and heat transfer variables during the first 2 sec from the beginning of the transient event for variations "3" and "4", respectively, which are examined in the present study. The number of cycles in the first 2 sec of each variation is different as it was expected.

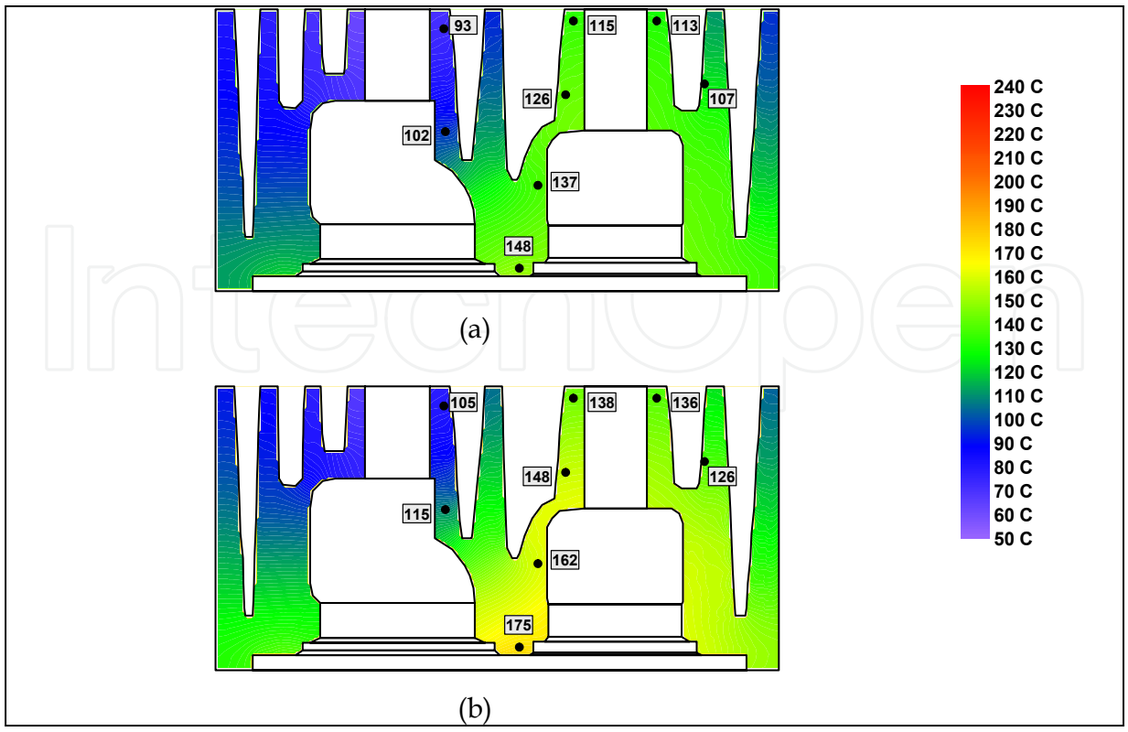

Fig. 7. Cylinder head temperature distributions, in deg. C, at the initial (a) and final (b) state of the load increment variation "1". Numbers in "squares" denote experimental temperature values taken from thermocouples.

The temporal response of cylinder pressure is presented for the two variations in Figs 8a and 9a, respectively. For variation "3", an increase of 1-1.5 bar is observed in the peak pressure during the first 3 cycles of the event. Variation in peak cylinder pressure becomes marginal after this moment, presents a slight fluctuation and reaches its final value almost 3 sec after initiation of the variation. For variation "4", the case is highly different from the previous one. Pressure changes rapidly and during the first four engine cycles after the beginning of the transient its peak value is increased linearly from 60 to 80 bar approximately. The 80 bar peak value is maintained afterwards almost constant for a period of slightly higher than 1 sec, when after approximately the 15th engine cycle it starts to decline in a slower pace to its final level of 70 bar which corresponds to the final steady state. The total time period the peak pressure demanded to settle in its final steady state value for this variation was evaluated to 5 sec. For both variations "3" and "4", the time instant after which peak pressure is settled to its final steady state value marks the end of the first phase of the thermal transient variation that was named as the "thermodynamic" one. As a result at the end of this phase, the combustion gas has reached its final steady state. The upcoming second phase of the transient thermal variation named as the "structural" one is expected to last much longer until all combustion chamber components have reached their temperatures corresponding to the final steady state. Additional details about these phases were provided by the author in (Rakopoulos and Mavropoulos, 1999, 2009). It is in general accepted that the duration of each period is primarily dependent on the respective duration and also on the magnitude

of speed and/or load change during each specific event. For the present case, the duration of "thermodynamic" phase is 3 sec for variation "3" and 5 sec for variation "4", respectively.

The time histories for the variation of measured wall surface temperature at the position of sensor HT#1 on cylinder head for the two transient events are presented in Figs 8b and 9b. In the same Figs they are observed the corresponding wall temperature variations for depths 1.0-3.0 mm below cylinder head surface inside the metal volume. The last variations were calculated using the modified one dimensional wall heat conduction model as described in 2.4. It is observed that wall surface temperature, as being a structural variable, continues to rise after 2 sec from the beginning of each transient event. However, this increase in surface temperature refers to its "long-term scale" variation and it is linear in the case of the moderate load increase of variation "3" (Fig. 8b), or exponential in the case of the ramp speed and load increase of variation "4" (Fig. 9b). By analysing the whole range of both experimental measurements it was concluded that the total duration of structural phase of the transient is estimated at 200 sec for variation "3", whereas it exceeds 300 sec in the case of variation "4". Similar values have been calculated theoretically by the author in the past using the simulation model for structural thermal field (Rakopoulos and Mavropoulos, 1999).

Of special importance are the results of measurements presented in Figs 8b and 9b related to the "short-term scale" that is with reference to the instantaneous cyclic surface temperatures. In the moderate load increase of variation "3", the amplitude of temperature oscillations remains essentially constant during the first 2 sec (and also during the rest of the event). On the contrary, in the case of the sudden ramp speed and load increase of variation "4", a gradual increase is observed in the amplitude of temperature oscillations during the first four cycles after the beginning of the transient following the corresponding increase of cylinder pressure in Fig. 9a. However, in the case of wall surface temperature (x=0.0), its peak values are presented rather unstable and amplitudes are far beyond the normal ones expected in the case of an aluminum combustion chamber surface. It is characteristic that the maximum amplitude of temperature oscillations as presented in Fig. 9b was 31 deg, which is inside the area of values observed in the case of ceramic materials in insulated engines (Rakopoulos and Mavropoulos, 1998). These extreme values of temperature oscillations is a clear indication of abnormal combustion, which occurs in the beginning of variation "4" and it likely lasts only for about 1.5 sec or the first 21 cycles after the beginning of the transient. After this period, surface temperature in the combustion chamber returns to its normal fluctuation and its amplitude is reduced to the value corresponding to the final steady state after approximately the 50th cycle from the beginning of the transient.

To obtain further insight into the mechanism of heat transfer during a transient operation, it is useful to examine the temporal development of temperature in the internal layers of cylinder wall up to a distance of a few mm below the surface. The results for the transient temperatures during variations "3" and "4" are presented in Figs 8b and 9b for values of depth x varying from 1.0-3.0 mm below the surface of the cylinder head. In Fig. 8b it is observed that for transient variation "3" there is no essential difference between the different engine cycles in each depth during the development of transient event. As expected the amplitude of temperature oscillations is highly reduced in the internal layers of

cylinder head volume and for x=3.0 mm below the combustion chamber surface practically there exists no temperature oscillation. On the other hand during transient variation "4" in Fig. 9b, the abnormal combustion indicated previously causes the development of a heat wave penetrating quickly in the internal layers of cylinder head. It is remarkable that during the first 20 cycles from the beginning of the event, temperature swings of 0.7 deg can be sensed even in a depth of x=3.0 mm below the surface of combustion chamber. The instant velocity of this penetration during the transient event "4" can also be estimated from the results presented in Fig. 9b. From the analysis of the results it was observed that the peak temperature in the depth of x=3.0 mm below the surface appears at an angle of 720 deg. As a consequence, during an approximate "time period" of 360 deg the thermal wave penetrates 3.0 mm inside the metallic volume of cylinder head. After the 20th cycle the temperature oscillations start to reduce and after a few more engine cycles are vanished in the depth of 3.0 mm below surface.

Following the above analysis for surface temperature, heat flux time histories for the point of measurement (HT#1) in the cylinder head and the two variations examined, are presented in Figs 8c and 9c. Heat flux histories are highly influenced by gas pressure and surface temperature variations, and their patterns are in general similar with them. In the case of variation "3", a mild increase in peak cylinder heat flux is observed during the first four cycles of the event and this is due to the similar increase observed in cylinder pressure during the same period. There is a marginal increase in peak values afterwards due to surface temperature increase and the final steady state peak value is reached after the 50th cycle, approximately. In variation "4", the heat flux is rather unstable following the pattern of surface temperatures. Due to the combustion instabilities described previously, measured peak heat flux values raised to almost three times higher than the ones observed during the normal engine operation, the highest of them reaching the value 9000 kW/m² corresponding to the same cycles in which the extreme surface temperature values have occurred. Peak heat flux is reduced afterwards at a slower pace to its final steady-state value, which is reached after the 200th cycle from the beginning of the event. A similar form of instantaneous heat flux variation during the first cycles of the warm-up period for a spark ignited engine was presented by the authors of (Wang & Stone, 2008).

5.4 Unsteady heat conduction phenomena in the engine gas exchange system

Phenomena related with the unsteady heat transfer in the inlet and exhaust engine manifolds are of special interest. In particular during the last years these phenomena have drawn special attention due to their importance in issues related with pollutant emissions during transient engine operation and especially the combustion instability which occurs in the case of an engine cold-starting event.

The variation of surface temperature and heat flux in the engine exhaust manifold follows in general the same trends as in the cylinder head. In this case, since the point of temperature and heat flux measurement was placed 100 mm downstream the exhaust valve (Figs 3 and 4), the corresponding phenomena are significantly faded out (Figs 10 and 11).

Increase of the amplitude of temperature oscillations is again obvious for variation "4" (Fig. 11a). However, there are no extreme amplitudes present in this case, as they have been absorbed due to the transfer of heat to the cylinder and manifold walls along the 100 mm distance from the exhaust valve to the point of measurement.

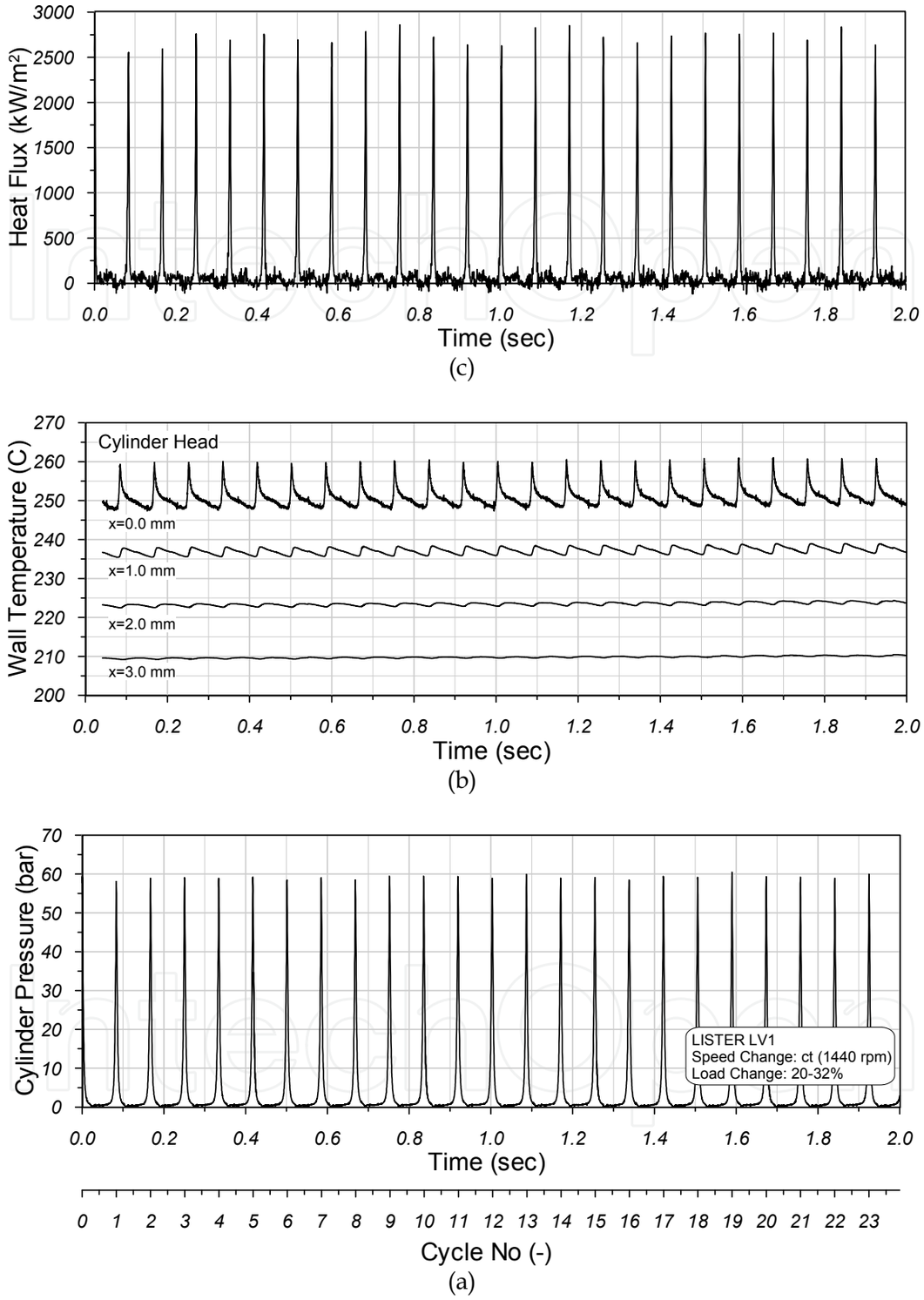

Fig. 8. Time histories of cylinder pressure (a), wall temperature for cylinder head on surface x=0.0 and three different depths inside the metal volume (b) and heat flux variation for cylinder head (c), for the first 2 sec of transient variation "3".

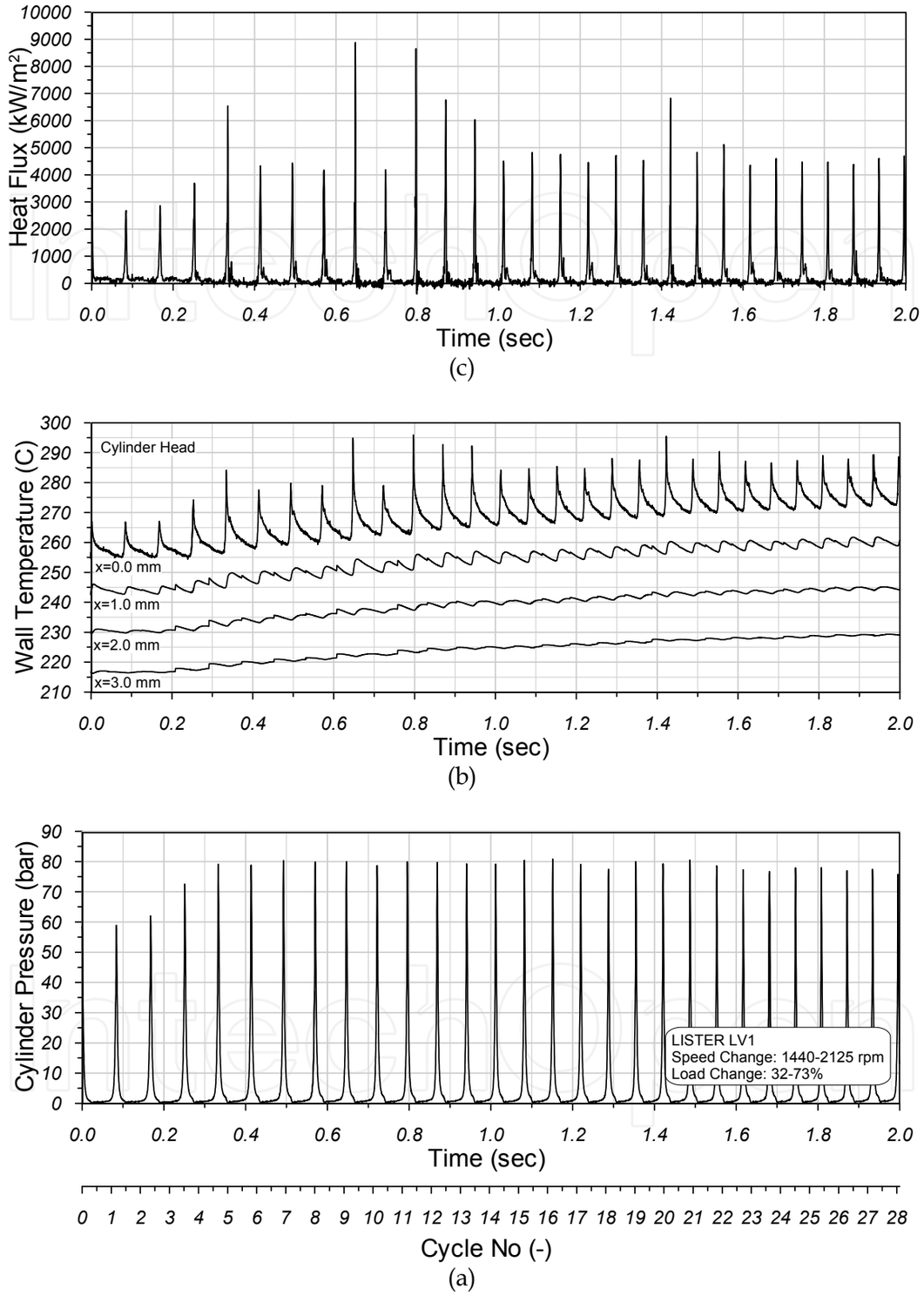

Fig. 9. Time histories of cylinder pressure (a), wall temperature for cylinder head on surface x=0.0 and three different depths inside the metal volume (b) and heat flux variation for cylinder head (c), for the first 2 sec of transient variation "4".

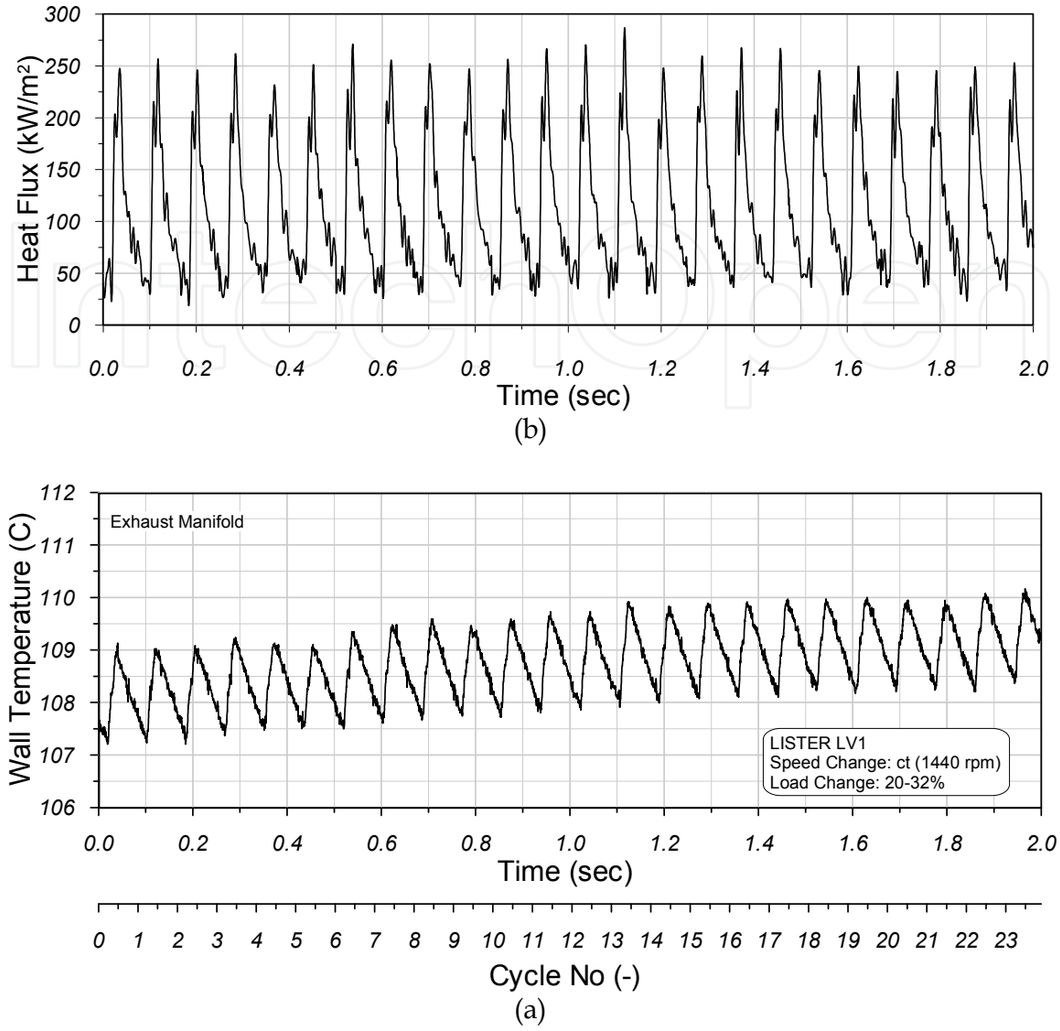

Fig. 10. Time histories of exhaust manifold wall surface temperature (a) and heat flux (b) at the position of sensor HT#4 for the first 2 sec of transient variation "3".

The corresponding results for heat flux time histories in the point of measurement on the exhaust manifold are presented in Figs 10b and 11b. In the case of variation "3", the moderate load increase is reflected as a marginal increase in exhaust manifold heat flux (a difference cannot be observed in time history of Fig. 10b). In the case of ramp variation "4" on the other hand, it is observed in Fig 11b a sudden increase in the amplitude of exhaust manifold heat flux, which starts 4 cycles after the beginning of the transient. In this case, there is no gradual increase of heat flux amplitude during the first four cycles, as it was the case for cylinder pressure and also cylinder head surface temperature and heat flux. Like the case of exhaust manifold surface temperature, this result is due to the heat transfer to combustion chamber and exhaust manifold walls until the point of measurement. It is observed that during the first 20 cycles of variation "4" the heat losses to exhaust manifold walls are increased beyond their normal level, due to increased engine speed and consequently gas velocity inside the exhaust manifold. The latter is the primary factor influencing heat losses in the exhaust manifold, as shown in (Mavropoulos et al., 2008). The

increased level of heat losses during the gas exchange period of each cycle for the first 20 cycles is the reason for the appearance of negative heat fluxes in the results of Fig. 11b. Such a case is quite remarkable and could not appear in the position of measurement during steady state operation. Heat flux becomes negative (that is heat is transferred from manifold wall to the gas) for a short period of engine cycle after TDC. This coincides with the period during which combustion gas temperature at the distance of 100 mm downstream the exhaust valve inside the manifold reaches its minimum value. The combination of instantaneous exhaust gas temperature with gas velocity at the point of measurement is the reason for the final result concerning the time history of heat flux in the exhaust manifold.

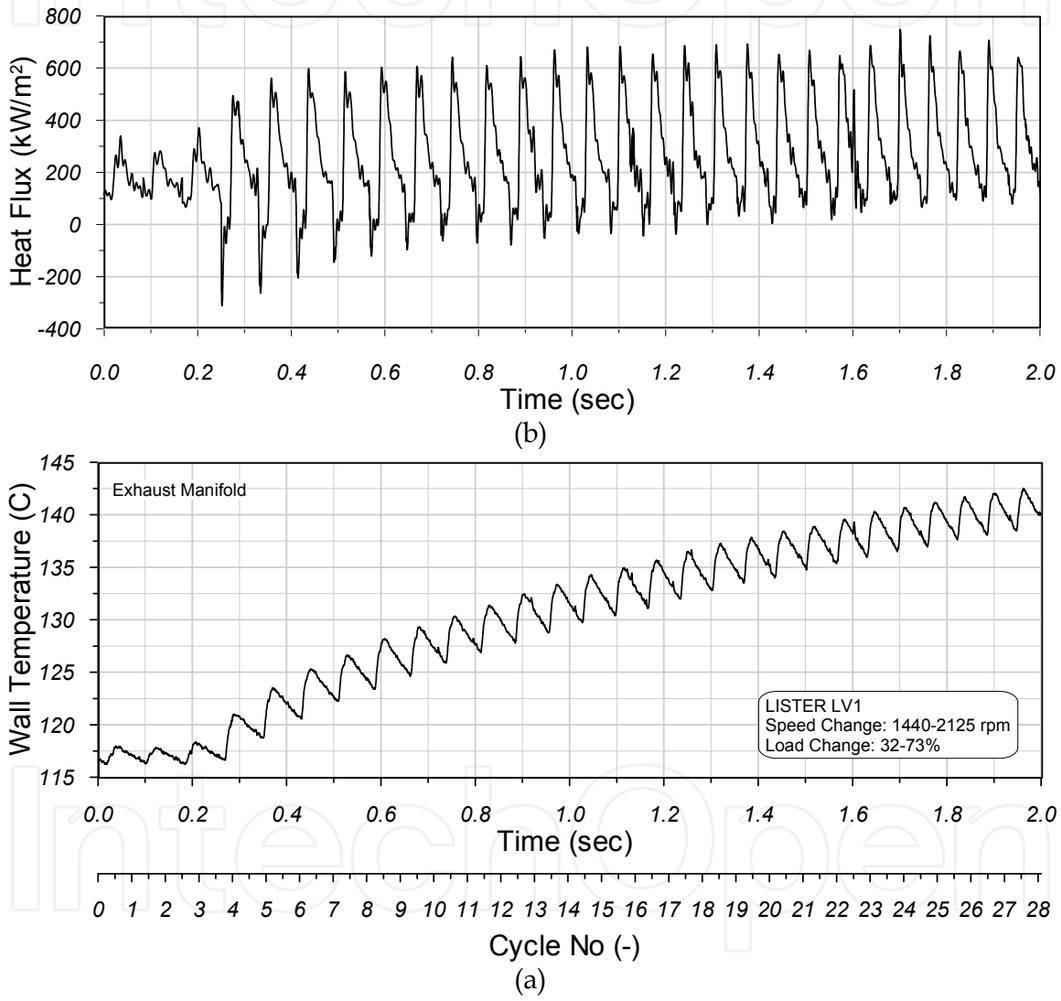

Fig. 11. Time histories of exhaust manifold wall surface temperature (a) and heat flux (b) at the position of sensor HT#4 for the first 2 sec of transient variation "4".

6. Conclusion

A theoretical simulation model accompanied with a comprehensive experimental procedure was developed for the analysis of unsteady heat transfer phenomena which occur in the combustion chamber and exhaust manifold surfaces of a DI diesel engine. The results of the

study clearly reveal the influence of transient engine heat transfer phenomena both in the engine structural integrity as well as in its performance aspects. The main findings from the analysis results of the present investigation can be summarized as follows:

- Thermal phenomena related to unsteady heat transfer in internal combustion engines can be categorized as long- or short-term response ones in relation to the time period of their development. Each long-term response variation is further separated to a "thermodynamic" and a "structural" phase.
- Calculated temperature profiles from the Finite Element sub-model matched satisfactorily the corresponding experimental temperature profiles recorded by the thermocouples, revealing that the area between the two valves (valve bridge) is the most sensitive one towards the generation of sharp temperature gradients during each transient (thermal shock). The effect of air velocity in the cooling procedure of external surfaces is clearly revealed and analysed.
- A strong influence exists between the long-term non-periodic heat transfer variation resulting from engine transient operation and the instantaneous cyclic short-term responses of surface temperatures and heat fluxes. The results of this interaction influence primarily the combustion chamber and secondary the exhaust manifold surfaces.
- In the first cycles ("thermodynamic" phase) of a ramp engine transient, abnormal combustion occurred. The result is that the amplitude of surface temperature swings and the peak heat flux value for cylinder head surfaces were increased at extreme values, reaching almost 3 times the level of the corresponding ones that occur during steady state operation.
- The respective phenomena inside the exhaust manifold at a distance of 100 mm downstream the exhaust valve have a minor impact on the local surfaces. Temperature gradients are reduced in low levels due to heat losses. The gas velocity inside the exhaust manifold is the main factor influencing heat transfer and wall heat losses.

7. References

Annand, W.J.D. (1963). Heat transfer in the cylinders of reciprocating internal combustion engines. *Proceedings of the Institution of Mechanical Engineers,* Vol.177, pp. 973-990

Assanis, D. N. & Heywood, J. B. (1986). Development and use of a computer simulation of the turbocompounded diesel engine performance and component heat transfer studies. *Transactions of SAE, Journal of Engines,* Vol.95, SAE paper 860329

Demuynck, J., Raes, N., Zuliani, M., De Paepe, M., Sierens, R. & Verhelst, S. (2009). Local heat flux measurements in a hydrogen and methane spark ignition engine with a thermopile sensor. *Int. J Hydrogen Energy,* Vol.34, No.24, pp. 9857-9868

Heywood, J.B. (1998). *Internal Combustion Engine Fundamentals,* McGraw-Hill, New York

Keribar, R. & Morel, T. (1987). Thermal shock calculations in I.C. engines, SAE paper 870162

Lin, C.S. & Foster, D.E. (1989). An analysis of ignition delay, heat transfer and combustion during dynamic load changes in a diesel engine, SAE paper 892054

Mavropoulos, G.C., Rakopoulos, C.D. & Hountalas, D.T. (2008). Experimental assessment of instantaneous heat transfer in the combustion chamber and exhaust manifold walls

of air-cooled direct injection diesel engine. *SAE International Journal of Engines,* Vol.1, No.1, (April 2009), pp. 888-912, SAE paper 2008-01-1326

Mavropoulos, G.C., Rakopoulos, C.D. & Hountalas, D.T. (2009). Experimental investigation of instantaneous cyclic heat transfer in the combustion chamber and exhaust manifold of a DI diesel engine under transient operating conditions, SAE paper 2009-01-1122

Mavropoulos, G.C. (2011). Experimental study of the interactions between long and short-term unsteady heat transfer responses on the in-cylinder and exhaust manifold diesel engine surfaces. *Applied Energy,* Vol.88, No.3, (March 2011), pp. 867-881

Perez-Blanco, H. (2004). Experimental characterization of mass, work and heat flows in an air cooled, single cylinder engine. *Energy Conv. Mgmt,* Vol.45, pp. 157-169

Rakopoulos, C.D. & Mavropoulos, G.C. (1996). Study of the steady and transient temperature field and heat flow in the combustion chamber components of a medium speed diesel engine using finite element analyses. *International Journal of Energy Research*, Vol.20, pp. 437-464

Rakopoulos, C.D. & Mavropoulos, G.C. (1998). Components heat transfer studies in a low heat rejection DI diesel engine using a hybrid thermostructural finite element model. *Applied Thermal Engineering,* Vol.18, pp. 301-316

Rakopoulos, C.D., Mavropoulos, G.C. & Hountalas, D.T. (1998). Modeling the structural thermal response of an air-cooled diesel engine under transient operation including a detailed thermodynamic description of boundary conditions, SAE paper 981024

Rakopoulos, C.D. & Hountalas, D.T. (1998). Development and validation of a 3-D multi-zone combustion model for the prediction of DI diesel engines performance and pollutants emissions. *Transactions of SAE, Journal of Engines,* Vol.107, pp. 1413-1429, SAE paper 981021

Rakopoulos, C.D. & Mavropoulos, G.C. (1999). Modelling the transient heat transfer in the ceramic combustion chamber walls of a low heat rejection diesel engine. *International Journal of Vehicle Design,* Vol.22, No.3/4, pp. 195-215

Rakopoulos, C.D. & Mavropoulos, G.C. (2000). Experimental instantaneous heat fluxes in the cylinder head and exhaust manifold of an air-cooled diesel engine. *Energy Conversion and Management*, Vol.41, pp. 1265-1281

Rakopoulos, C.D., Rakopoulos, D.C., Giakoumis, E.G. & Kyritsis, D.C. (2004). Validation and sensitivity analysis of a two-zone diesel engine model for combustion and emissions prediction. *Energy Conversion and Management,* Vol.45, pp. 1471-1495

Rakopoulos, C.D. & Mavropoulos, G.C. (2008). Experimental evaluation of local instantaneous heat transfer characteristics in the combustion chamber of air-cooled direct injection diesel engine. *Energy,* Vol.33, pp. 1084–1099

Rakopoulos, C.D. & Mavropoulos, G.C. (2009). Effects of transient diesel engine operation on its cyclic heat transfer: an experimental assessment. *Proc. IMechE, Part D: Journal of Automobile Engineering,* Vol.223, No.11, (November 2009), pp. 1373-1394

Sammut, G. & Alkidas, A.C. (2007). Relative contributions of intake and exhaust tuning on SI engine breathing-A computational study, SAE paper 2007-01-0492

Wang, X. and Stone, C.R. (2008). A study of combustion, instantaneous heat transfer, and emissions in a spark ignition engine during warm-up. *Proc. IMechE,* Vol.222, pp. 607-618

Wu, Y., Chen, B., Hsieh, F. & Ke, C. (2008). Heat transfer model for scooter engines, SAE paper 2008-01-0387

Heat Transfer - Engineering Applications
Edited by Prof. Vyacheslav Vikhrenko

ISBN 978-953-307-361-3
Hard cover, 400 pages
Publisher InTech
Published online 22, December, 2011
Published in print edition December, 2011

Heat transfer is involved in numerous industrial technologies. This interdisciplinary book comprises 16 chapters dealing with combined action of heat transfer and concomitant processes. Five chapters of its first section discuss heat effects due to laser, ion and plasma-solid interaction. In eight chapters of the second section engineering applications of heat conduction equations to the curing reaction kinetics in manufacturing process, their combination with mass transport or ohmic and dielectric losses, heat conduction in metallic porous media and power cables are considered. Analysis of the safety of mine hoist under influence of heat produced by mechanical friction, heat transfer in boilers and internal combustion engine chambers, management for ultrahigh strength steel manufacturing are described in this section as well. Three chapters of the last third section are devoted to air cooling of electronic devices.

InTech Europe
University Campus STeP Ri
Slavka Krautzeka 83/A
51000 Rijeka, Croatia
Phone: +385 (51) 770 447
Fax: +385 (51) 686 166
www.intechopen.com

InTech China
Unit 405, Office Block, Hotel Equatorial Shanghai
No.65, Yan An Road (West), Shanghai, 200040, China
中国上海市延安西路65号上海国际贵都大饭店办公楼405单元
Phone: +86-21-62489820
Fax: +86-21-62489821

IntechOpen